Nucleic Acids Research, 1998, Vol. 26, No. 6 **1473–1480**

Study of the interaction of DNA with cisplatin and other Pd(II) and Pt(II) complexes by atomic force microscopy

G. Bibiana Onoa, Gemma Cervantes, Virtudes Moreno* and M. José Prieto[1]

Departament de Química Inorgànica, Universitat de Barcelona, Diagonal 647, 08028-Barcelona, Spain and [1]Departament de Microbiología, Universitat de Barcelona, Diagonal 645, 08028-Barcelona, Spain

Received October 31, 1997; Revised and Accepted January 29, 1998

ABSTRACT

Modifications in the structure of a 260 bp DNA (*hlyM*) fragment from *Escherichia coli* caused by interaction with Pd(II) and Pt(II) complexes were studied. Cisplatin and transplatin [*cis*- and *trans*-$PtCl_2(NH_3)_2$ respectively], $Pt_2Cl_2(Spym)_4$ (Spym = 2-mercaptopyrimidine anion), Pd-famotidine and Pt-famotidine were incubated with DNA for 24 h at 37°C and then observed with an atomic force microscope. Atomic force microscopy (AFM) provides the opportunity for nanometer resolution in research on the interaction between nucleic acids and metal complexes. The complexes induced noticeable changes in DNA topography according to their different characteristics and structure. In the case of cisplatin a shortening in DNA strands was observed. Transplatin and $Pt_2Cl_2(Spym)_4$ caused shortening and compaction, whilst an aggregation of two strands was observed for the Pt-famotidine compound but not for the Pd-famotidine compound or the metal-free famotidine.

INTRODUCTION

Cisplatin and carboplatin, first and second generation platinum drugs respectively, are well known as anti-tumour agents used in clinical treatments (1–7). The mode of action of cisplatin inside the cell has been investigated since its discovery. It is known that the target of the metal complex is DNA (8–11) and that the nitrogen atoms of the bases, mainly N_7 of guanine, are bound to the platinum following hydrolysis of the chloride ions inside the cell nucleus (12–15). The success of cisplatin in cancer chemotherapy derives from its ability to crosslink DNA and alter DNA structure. Native DNA is distorted by cisplatin, which binds covalently to both linear and circular DNA forms. The degree of coiling is probably altered by disruption and unwinding of the double helix. Base stacking is disrupted and adduct formation is localized in the major groove. Some structural changes, such as the development of kinks and shortening, may occur. These modifications have already been observed in circular DNA by electron microscopy (16–18) and in linear DNA by atomic force microscopy (AFM) (19,20). Carboplatin is an analogue of cisplatin and its mode of action is similar to that of cisplatin (22–23). New Pt(II) and Pt(IV) drugs, which are less toxic than cisplatin, have been developed (3,7). Different types of platinum complex have been produced and some have been tested successfully as active anti-tumour agents (23–27). We have previously synthesized and studied several new palladium and platinum compounds (27–29). The interaction of some of these complexes with circular plasmid DNA or linear calf thymus DNA has been followed by several techniques, such as UV spectroscopy, circular dichroism (CD), electrophoretic mobility, melting point determination and electron microscopy (28,29). The results indicated changes in the structure of DNA, probably due to covalent interactions between the metal ions and bases. However, correlations between the structure and the mode of interaction could not be established.

Biological AFM is a rapidly developing interdisciplinary field of research (30–34). Several improvements have been made since 1992, when Bustamante *et al*. published the first credible DNA images by AFM in air (35) with a resolution comparable with that of conventional electron microscopy. AFM has been used for imaging of single-stranded DNA, double-stranded DNA, DNA–protein complexes and DNA–metal complexes (19,20,36–39). In 1992 Rampino (20) observed, using AFM, that cisplatin induced geometric irregularities, in the form of kinks and width distortions, in oriented fibres of DNA. In 1993 Jeffrey *et al*. (19) identified DNA–cisplatin adducts by scanning tunneling microscopy (STM). Tapping mode AFM (TMAFM) has become a powerful technique that combines some of the advantages of contact and non-contact AFM. TMAFM minimizes the lateral forces as well as the interaction time with the sample (40,41). We have used TMAFM in order to establish differences in the modes of interaction between DNA and the set of Pt(II) and Pd(II) complexes shown in Figure 1: cisplatin (CDDP), transplatin (TDDP), 2-mercaptopyrimidine (Spym), Pt-mercaptopyrimidine (Pt-Spym), famotidine (fam), Pd-famotidine (Pd-fam) and Pt-famotidine (Pt-fam). These have different structures and are promising anti-tumour agents (27–29).

MATERIALS AND METHODS

Materials

Cisplatin and transplatin were purchased from Johnson Matthey (Royston, UK) and the other complexes were prepared as previously described (27–29) using K_2PdCl_4 or K_2PtCl_4 (Johnson Matthey). Famotidine, 2-mercaptopyrimidine, Tris, boric acid

*To whom the correspondence should be addressed. Tel: +34 3402 1225; Fax: +34 3490 7725; Email: vmoreno@kripto.qui.ub.es

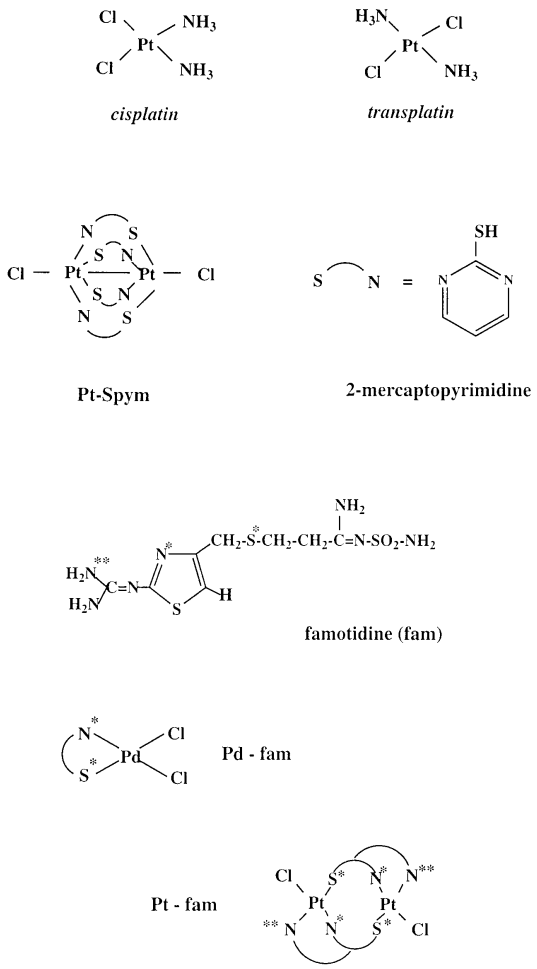

Figure 1. Schematic representation of the ligands and complexes used for DNA modification.

and HEPES were obtained from ICN (Barcelona, Spain) without further purification. EDTA and TRIZMA hydrochloride were purchased from Sigma (Madrid, Spain); NaCl, KOH and $MgCl_2$ from Merck (Madrid, Spain); ammonium persulfate from BioRad (Madrid, Spain); TEMED from Serva (Barcelona, Spain). Ultrapure agarose was obtained from ECOGEN (Barcelona, Spain) and electrophoresis grade acrylamide and bis(acrylamide) from BioRad (Madrid, Spain).

Isolation of *hlyM* DNA

hlyM DNA is a 260 bp fragment from the hemolysin operon of *Escherichia coli*, which was amplified by PCR (GeneAmp PCR system 2400; Perkin-Elmer Cetus) and purified with a Wizard Clean-up System kit (Promega, Madrid, Spain). The sequence of this fragment was previously selected in order to obtain a high guanine content and ensure binding of metallic complexes, since platinum preferentially binds to the N_7 atom of guanine (42). The purity and concentration of the DNA was verified by electrophoretic mobility in a 1% agarose gel slab with TBE running buffer. The marker used was ϕX174-*Hae*III (Promega, Madrid, Spain). Following this the DNA was diluted in HEPES buffer [40 mM HEPES, 10 mM $MgCl_2$, pH 7.2 (KOH)] (43) at a concentration of 5 ng/ml.

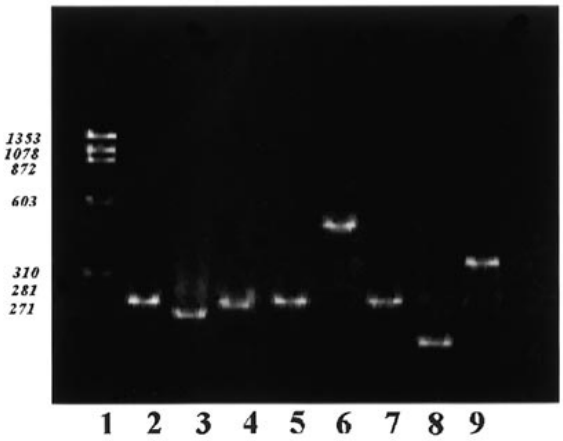

Figure 2. Comparison of the migration of metallic and non-metallic complexes on a non-denaturing 8% polyacrylamide gel. (Left) Lane 1, ϕX174, the marker; lane 2, free *hlyM* DNA; lane 3, DNA incubated with cisplatin; lane 4, DNA incubated with transplatin; lane 5, DNA incubated with Spym; lane 6, DNA incubated with Pt-Spym; lane 7, DNA incubated with fam; lane 8, DNA incubated with Pd-fam; lane 9, DNA incubated with Pt-fam. Samples were incubated for 24 h at 37°C.

Preparation of adducted DNA–metal complexes

Cisplatin and transplatin adducts. Fifteen nanograms of *hlyM* DNA was incubated in an appropriate volume with the required platinum concentration corresponding to the molar ratio $r_i = 0.5$. Cisplatin and transplatin complexes were dissolved in HEPES buffer and passed through 0.2 nm FP030/3 filters (Scheicher & Schueell GmbH, Germany). The reactions were run at 37°C for 24 h in the dark.

Other adducts. The samples were prepared as described above but the complexes were dissolved in a DMSO, HEPES (30:70) mixture, since they are only slightly soluble in HEPES buffer. In order to check the purity of the adducts formed, as well as the structural changes occurring in the DNA, the ligated complexes were run on an 8% polyacrylamide gel [acrylamide:bis (acrylamide) 29:1; 90 mM Tris–borate, 2 mM EDTA, pH 8.0; 0.2% ammonium persulfate and TEMED]. The voltage applied was 7 V/cm. Electrophoresis was performed at room temperature. The compounds were dissolved in buffer (10 mM TRIZMA, 0.1 mM EDTA, 50 mM NaCl, pH 7.4) or in a DMSO, TE (30:70) mixture, maintaining the r_i values described above.

Sample preparation for atomic force microscopy

Samples were prepared by placing a drop (2 µl) of DNA solution or DNA–metal complex solution onto freshly cleaved green mica (Ashville-Schoonmaker Mica Co., Newport News, VA). After adsorption for 5 min at room temperature the samples were rinsed for 10 s in a jet of deionized water of 18 MΩ/cm from a Milli-Q water purification system (Millipore, Molshem, France) directed onto the surface with a squeeze bottle. The samples were dried with a stream of compressed argon over silica gel for 30 min before imaging in the AFM. Sometimes small amorphous precipitates appeared in the images obtained by AFM, due to the Mg HEPES buffer (42,43). The use of a high pressure water rinse or avoidance of this buffer and the use of water only are thus recommended. However, an undesirable effect may be observed, with a decrease of about one order of magnitude in the amount of DNA bound to the

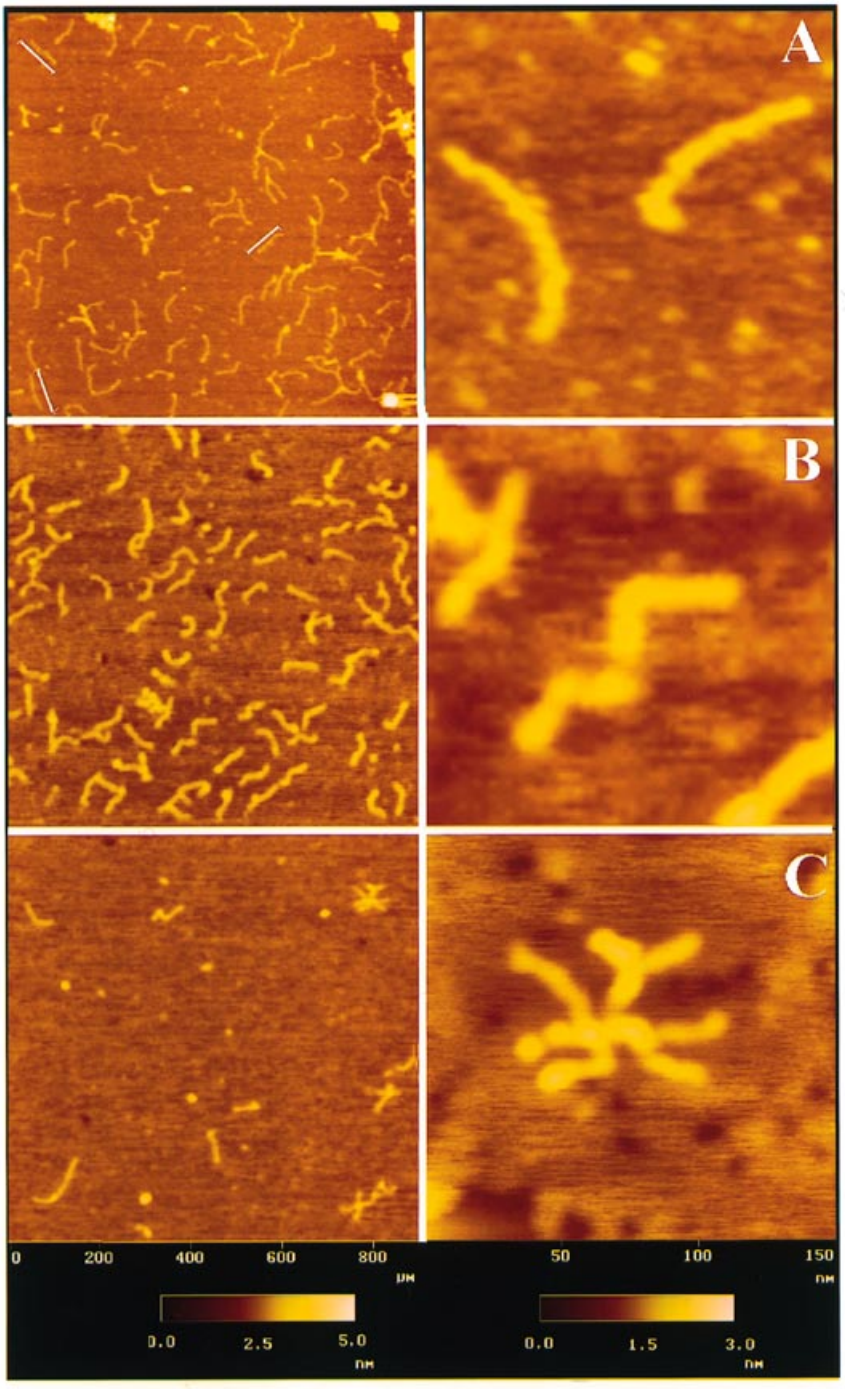

Figure 3. (**A**) TMAFM images in dry air of a 260 bp linear fragment of *hlyM* double-stranded DNA in HEPES, $MgCl_2$ buffer at a concentration of 0.5 ng/µl adsorbed on bare mica. Lines were drawn along the molecule in order to measure the length of the fragment. Measurements are summarized in Table 1. (**B**) TMAFM images in dry air of the adducts of *hlyM* double-stranded DNA with dichlorodiammin platinum(II) complexes incubated for 24 h at 37°C with a ratio of 1 Pt atom/2 bp DNA. *hlyM* with cisplatin, shortening 30%. (**C**) *hlyM* with transplatin under the same conditions. Height information is coded in colour according to the horizontal bars. The scan sizes are 1000 ×1000 nm (left overview) and 150 ×150 nm (right zoom).

mica (44). In this study Mg HEPES buffer was used and a few patches appeared in some of the images.

Atomic force microscopy

The samples were imaged in a Nanoscope III Multimode AFM (Digital Instrumentals Inc., Santa Barbara, CA) operating in tapping mode in air (40,41) at a scan rate of 1–3 Hz. The AFM probes were 125 µm long monocrystalline silicon cantilevers with integrated conical Si tips (Nanosensors GmbH, Germany) with an average resonance frequency $f_0 \approx 330$ kHz and a spring constant $K \approx 50$ N/m. The cantilever is rectangular with a tip radius given by the suplier of ~5 nm, a cone angle of 35° and a high aspect ratio. In general the images were obtained at room

temperature (T = 23 ± 2°C) and the relative humidity (RH) was typically 55%. Only a few rigorous studies on DNA imaged in AFM at different humidities have been reported (35,45).

Apparent contour lengths of DNA strands were measured in top view images. Although in some images there was considerable end-to-end aggregation of molecules, only the molecules within ~20% of the expected length were measured. Mean apparent heights of DNA were measured using the Bearing command in the Nanoscope software and were verified with Section-Cursor-Average. All the heights were measured between the top of the biomolecules and the average height of the underlying substrate. The mean apparent width was also measured with the Bearing command of Nanoscope III v.4.1 (43). Each sample was imaged in different places and many times in order to obtain reliable measurements.

Statistical analysis

The differences in length and height between the DNA complexes and free DNA were compared by a non-parametric analysis (Kruskal–Wallis Z). The statistical treatment was performed by means of the SOLO® Statistical Package (BMDP Statistical Sofware Inc., Los Angeles, CA). A P value of 0.05 was considered significant.

RESULTS AND DISCUSSION

Effects on gel electrophoretic mobility of DNA species

Previous reports (16–20,28) have demonstrated that a platinum complex induces several changes in DNA conformation after the complex has been bound. Electrophoretic mobility of free DNA can be increased or decreased by metal complexes, which could induce DNA deformations, such as bending, 'local denaturation' (overwinding and underwinding), microloop formation and subsequent DNA shortening. Figure 2 shows the results of migration of metallic and non-metallic adducts with *hlyM* DNA incubated at 37°C for 24 h. Most of the metallic complexes change the DNA conformation considerably. Electrophoretic mobility increases after incubation with cisplatin (slot 3), consistent with previous reports on circular DNA (16,19). The increase in electrophoretic mobility of cisplatin–DNA adducts suggests that hydrogen bonds are disrupted, which causes localized unwinding of the duplex. The interruption of base pairing would produce single-stranded regions that under the gel conditions would collapse and shorten the DNA.

In the case of transplatin–DNA complexes the electrophoretic mobility is close to that observed in free DNA. From several experiments a slightly higher mobility was estimated, but this is not enough to suggest noticeable shortening of DNA molecules after the complex is bound.

No significant changes in the electrophoretic mobility were observed in DNA after incubation with non-metallic compounds, as expected. Electrophoretic mobility of the Pt-Spym–DNA adduct was less than that of free DNA. DNA migration rates through the gel are inversely proportional to the logarithm of the number of base pairs, but in large DNA fragments a great decrease in migration can be observed. In this case aggregation giving larger DNA fragments is probable if the geometry of the complex is taken into account. The gel electrophoretic mobility of Pd-fam–DNA and Pt-fam–DNA adducts increases and decreases respectively. The results suggest that binding of Pd-fam introduces conformational changes in DNA fragments as well as shortening, while Pt-fam induces aggregation of DNA molecules.

Table 1. Dimensions of the molecules (defined in Figs 2 and 5–7) obtained from TMAFM

Adducts	Length (nm)	Height (nm)	Width (nm)
DNA	87 ± 6.5	0.45 ± 0.06	10.2 ± 0.7
DNA–CDDP	68 ± 9.0	0.35 ± 0.15	13.1 ± 0.6
DNA–TDDP	67 ± 7.2	0.45 ± 0.07	16.4 ± 2.1
DNA–Spym	86 ± 12	0.57 ± 0.10	11.8 ± 0.6
DNA–Pt-Spym	[a]	0.86 ± 0.16	30.1 ± 6.3
DNA–fam	77 ± 7.9	0.50 ± 0.07	14.6 ± 0.6
DNA–Pd-fam	28 ± 20	1.57 ± 0.38	[b]
DNA–Pt-fam	64 ± 12	0.74 ± 0.16	22.2 ± 3.5

n, number of molecules measured per image. Errors are ±1 standard deviation.
[a]Length was not measured due to aggregation of molecules.
[b]The measurements of apparent width and length are equal, i.e. oblate shape.

DNA and DNA complex images

Linear *hlyM* DNA incubated at 37°C for 24 h is shown in representative images in Figure 3A. The overview image contains a large number of linear and curved molecules (top left). Some relevant morphological features can be observed in the magnification (top right). Lengths, widths and heights for fully extended DNA molecules are shown in Table 1. A distribution of the sizes measured is presented in Figure 4. The mean contour length was 87 nm, which corresponds to a helical rise of 0.34 nm/bp, that expected for B-form DNA (46). The mean apparent width of the DNA was larger than 2.4 nm (the intrinsic width of DNA due to the radius of the contacting tip and to the large adhesion forces). The apparent lateral dimensions of the molecules can be calculated according to (35)

$$W = 4(R_c + R_m)\,[R_m(R_c - R_m)]^{1/2}/R_c$$

where R_c = 5 nm (expected tip radius) and R_m = 1.2 nm (DNA helix radius). The expected width was 10.5 nm, which is also close to the width measured. The height data obtained were <2 nm and are consistent with reported heights of dried DNA (35,42,47,48). In Figure 5A it can be observed that most of the molecules measured had similar heights. Only a few of them had higher values. A total of 41% of the measured samples had a height of between 0.4 and 0.6 nm. The experimental results are consistent with the theoretical prediction.

It has been shown that 99.5% of cisplatin is bound to DNA after incubation for 24 h at 37°C, producing the changes mentioned above (49). An image of a *hlyM* DNA fragment incubated with cisplatin under similar conditions is shown in Figure 3B. The molecules are shorter and more compact, as found in earlier studies (16–20). These features are also confirmed by the electrophoretic mobility (Fig. 2). The average lengths, widths and heights measured are shown in Table 1 and compared in Figure 5. In contrast to the values obtained by Jeffrey *et al*. (19), we observed a shortening of the DNA fragment (±30%), probably due to the ability of cisplatin to crosslink DNA. Microkinks are also probably formed and contribute to shortening of the fragments, although no significant microloop- or local denaturation-like

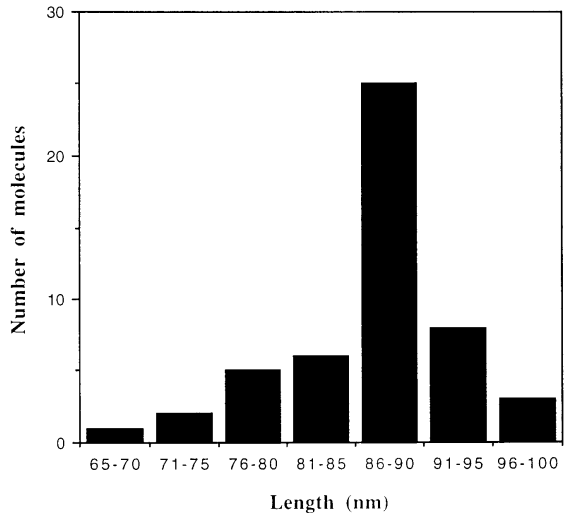

Figure 4. Quantitative image analysis of TMAFM images. Histogram of the mean apparent contour length measured from free *hlyM* DNA fragments. The average length ± standard deviation was 87 ± 6.5 nm for 50% of the population measured.

structures were apparent. These results are consistent with that obtained for circular DNA (16–18).

Figure 3C shows images corresponding to samples of the *hlym* DNA fragment incubated with transplatin under the same conditions as for cisplatin in Figure 3B. Transplatin, like cisplatin, passes into cells and binds to DNA (50,51). However, transplatin inhibits DNA replication only at higher doses than cisplatin. There are several explanations for this phenomenon, including different cellular uptake of the two isomers and/or repair of their DNA adducts (9,23,42). The concentration of DNA molecules is considerably less due to the water rinse conditions. In the images there are both single molecules and aggregates. It is known that monofunctional adducts formed by cisplatin and transplatin can further react with N sites from bases of the same strand, to form intrastrand bifunctional crosslinks, or bases of the opposite strand and/or with proteins, to form interstrand crosslinks and DNA–protein crosslinks respectively. In addition, transplatin binds less selectively than the *cis* isomer (9). On the other hand, Butourd and Johnson (52) reported that monoadducts formed on double-stranded DNA by transplatin, with a half-life of 30 h at 37°C, are much longer lived than those formed by cisplatin. Biological processing of long-lived monofunctional adducts could account for the different activities of the two isomers. Eastman and Barry (53) also reported that only 50% of transplatin monoadducts have been closed after 24 h reaction with double-stranded DNA. In our case the single molecules that were shorter than free DNA (see Table 1 and Fig. 5B) could correspond to adducts formed. Statistical analysis shows that the DNA molecules underwent a similar shortening after incubation with either complex, cisplatin or transplatin.

Figure 6 shows images corresponding to samples of the same *hlyM* DNA incubated for 24 h at 37°C with platinum-free 2-mercaptopyrimidine (see Fig. 1) and the Pt-Spym complex respectively. The latter compound is an inhibitor in HeLa (human womb carcinoma) and HL60 (human leukemia) cells (28). In Figure 6B a slight increase in the width of the strands in relation to the other measurements (Table 1) can be observed. The most noticeable phenomenon is the formation of aggregates, confirmed by a significant decrease in electrophoretic mobility. Single molecules were not observed in the images. Thus binding of Pt-Spym induces an interaction between different DNA strands. It probably binds through the two lateral sites after the Pt–Cl bond has been hydrolyzed. The effect observed is not due to the ligand. The effect of 2-mercaptopyrimidine on DNA under the same conditions is shown in Figure 6A. The length of the strands did not change (see Fig. 5B). Early (CD) and electrophoretic studies carried out with famotidine and its metal complexes for a similar platinum:nucleotide ratio showed behaviour that was consistent with the structural changes observed using TMAFM (detailed CD and electrophoretic studies on famotidine and its metal complexes will be published shortly). In general, these studies show that free famotidine does not modify the secondary structure of DNA; famotidine-platinum(II) produces uncoiling of the double helix and

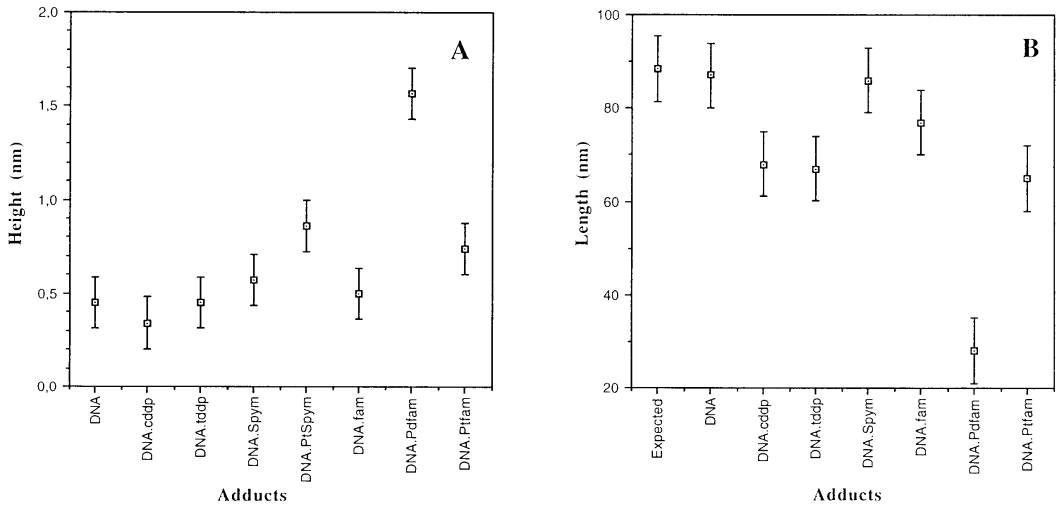

Figure 5. Error bar graphs of the standard deviation from the mean for each DNA adduct imaged by AFM in air. (**A**) Comparison between mean apparent heights of the different samples imaged. The adduct formed by Pd-fam shows the largest value of average heights, 1.56 nm. (**B**) Comparison between mean apparent contour lengths of the different samples imaged and expected DNA length. Cisplatin–, transplatin–, Pd-fam– and Pt-fam–DNA adducts show the most noticeable differences, consistent with the results from a Kruskal–Wallis *Z* value test.

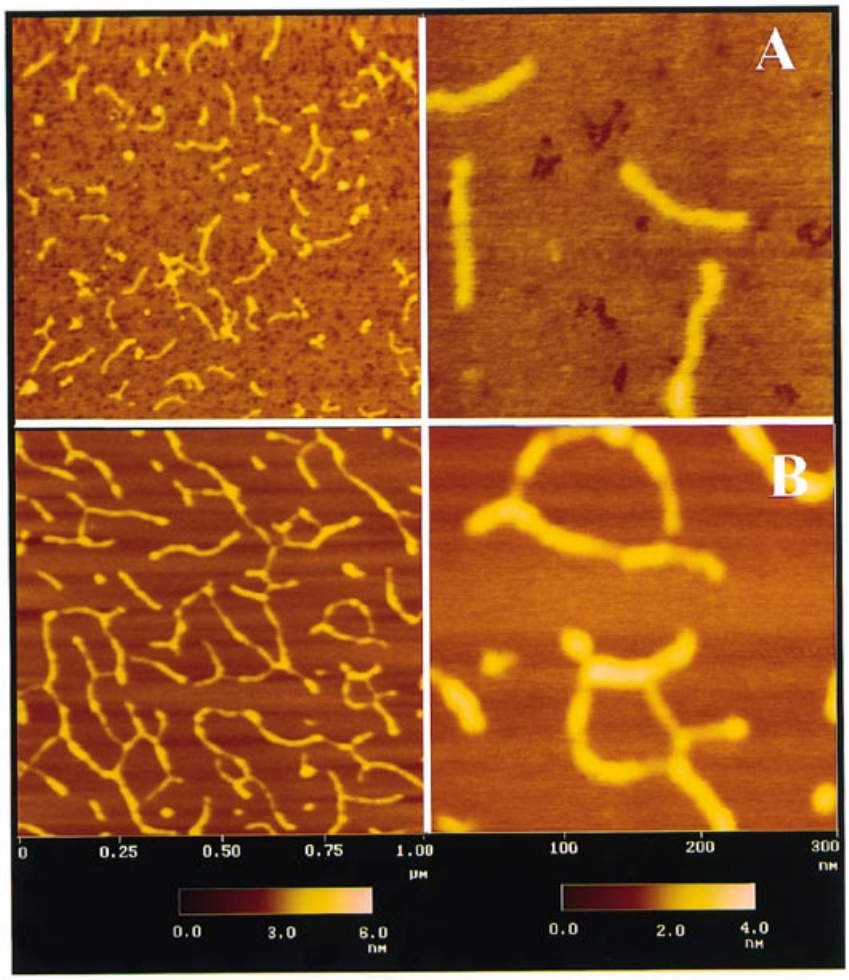

Figure 6. TMAFM images in dry air of the adducts of *hlyM* double-stranded DNA with (**A**) platinum-free 2-mercaptopyrimidine for 24 h at 37°C at a molar ratio of 0.5 and (**B**) Pt-Spym for 24 h at 37°C at a molar ratio of 0.5.

famotidine-palladium(II) induces compaction of the molecules due to changes in base stacking.

Figure 7A shows *hlyM* DNA incubated with famotidine. It can be observed that two or more molecules are bound. This is probably because free famotidine could interact with the DNA helix through hydrogen bonds, since its own structure offers many possible sites for this kind of interaction. The lengths, widths and heights are shown in Table 1 and Figure 5. They did not show significant changes in relation to free DNA. In the case of the famotidine-palladium(II) complex a significant modification of the DNA can be observed (Fig. 7B). The DNA has lost its filamentous structure and been converted to oblate structures. Different samples were imaged to ensure that imaging was free from artefacts. It is possible that the oblates could correspond to compacted DNA molecules, as suggested by the following. *A priori* the DNA fragment has a cylindrical geometry ~2 nm in diameter and ~86 nm in length. This fragment has a volume of ~271 nm^3. If the fragment was compacted and converted into an oblate, the volume would be the same, but the diameter would change. The new diameter would be ~8 nm. As discussed above, if the effects of the tip radius are considered, the length or diameter expected would be ~14.4 nm. Statistical analysis shows that 52% of the molecules measured have a length close to the value expected. This differs from the average indicated in Table 1 and Figure 5B, since it was plotted considering the whole population. It is probable that the other larger oblates observed in the image will correspond to aggregates.

Another interesting feature is the noticeable difference in the height of these molecules. In Figure 5A it can be observed that the height of the DNA–Pd-fam adducts is greatest. This is not surprising, since the DNA has been compacted and its molecular radius has increased. The results are consistent with the changes observed by CD in calf thymus DNA incubated with Pd-fam. This behaviour could be due to an intrastrand mode of binding to DNA, which is likely, given the structure of the complex as determined by X-ray analysis (Fig. 1).

The Pt complex is a dimer and its mode of binding is quite different. In this case an interstrand mode of binding to DNA is possible and, therefore, aggregation of several strands can be induced, as shown in Figure 7C. The single molecules observed for the adduct were shorter than those of platinum-free fragments (Table 1 and Fig. 5B). Bending alongside the strand and a slight increase in width was also observed. These effects could be due to covalent bonds between the metal ions and N atoms of the

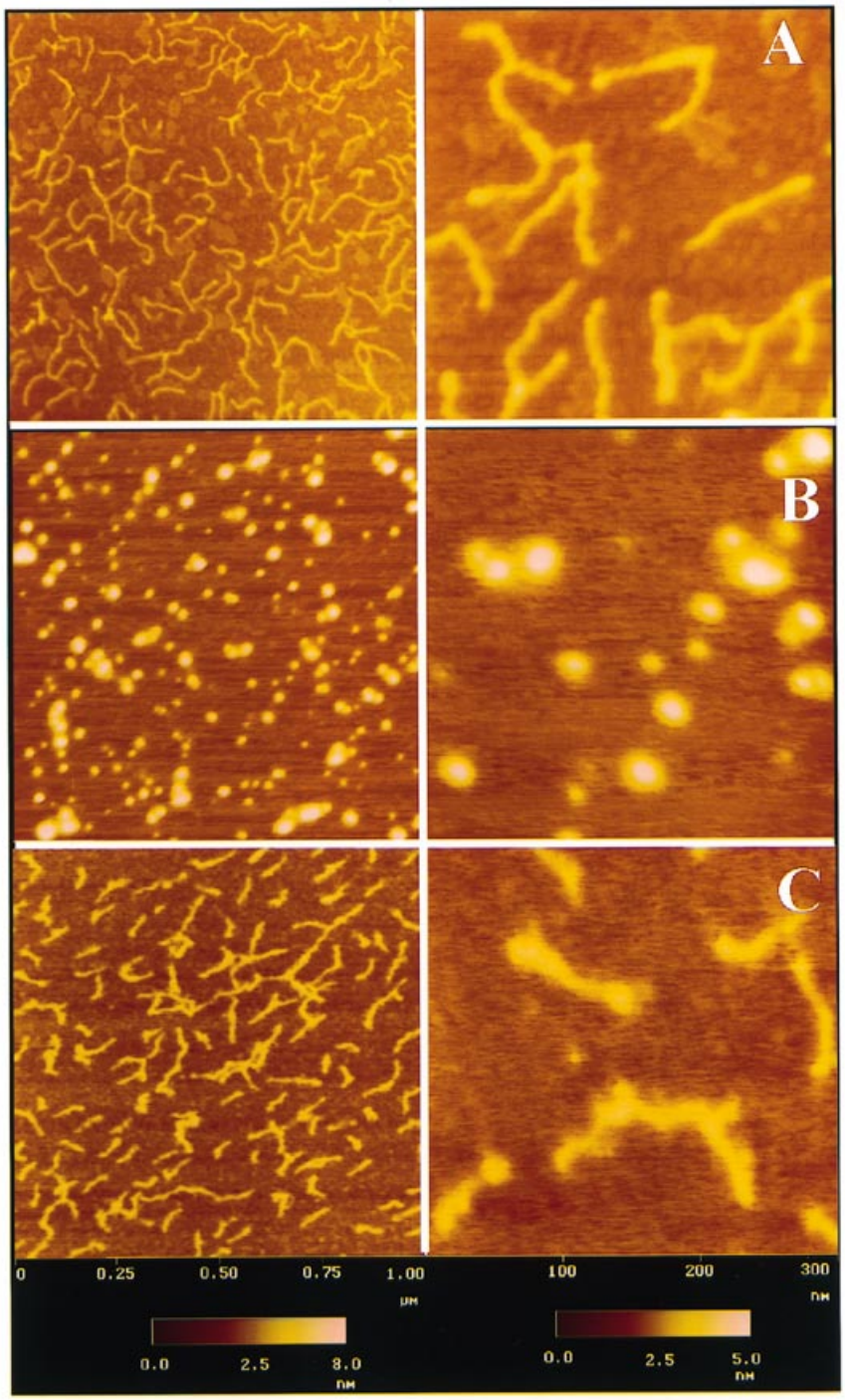

Figure 7. Selection of TMAFM images from different runs of *hlyM* DNA incubated with famotidine and the famotidine–metal complexes for 24 h at 37°C at a molar ratio of 0.5. Comparison of (**A**) *hlyM* DNA with metal-free famotidine, (**B**) *hlyM* DNA complexed with Pd-fam and (**C**) *hlyM* DNA complexed with Pt-fam.

bases, which are typically responsible for the contraction and compaction of DNA molecules, although aggregation would be the main phenomenon observed in all the samples imaged. The mean contour length in the larger individual fragments was 211 nm. This feature was also shown by retardation in gel mobility.

In conclusion, the use of TMAFM enables identification of modifications in DNA development on the surface caused by Pt or Pd complexes. These results are consistent with the changes observed in electrophoretic mobility. We have obtained image evidence that linking to small metallic complexes can change the DNA conformation significantly. These changes are related to the different structures of the complexes, which determine their mode of binding to DNA. We have also shown that the metals play an important role, since no changes in DNA conformation were observed with metal-free ligands. The most noticeable changes observed in the DNA molecules were in morphology and length

(shortening or aggregates). The multiple comparison test demonstrated that the DNA length was significantly different from that of DNA–cisplatin, –transplatin, –Pd-fam and –Pt-fam adducts. The measured height of DNA was different from that of DNA–Pd-fam, –Pt-fam and –Pt-Spym complexes (G.B.O., G.C., V.M. and M.J.P., unpublished results). The anti-tumour activity of one of these platinum complexes, cisplatin, is well known. A study of anti-tumour behaviour of the other Pd and Pt compounds is in progress. The results presented here suggest that they are also promising anti-tumour agents. The target for all of these metal compounds is DNA and, as observed here, interaction leads to modifications of DNA conformation. TMAFM offers significant potential for studying these, because the tip touches the sample and the resolution is almost as good as that in contact mode. However, the damage caused by shear forces during scanning is considerably reduced because the contact is brief. One disadvantage is that in order to obtain reliable images free of artefacts great care must be taken to obtain samples of high purity. Double-distilled water should be used to rinse the samples and special precautions should be taken when drying them, to prevent contamination of the background. Imaging of DNA–metallic complexes in air is easy and reliable, which is important in order to improve our understanding of how cisplatin cytotoxity (and that of other drugs) is mediated.

ACKNOWLEDGEMENTS

We are grateful to Pau Gorostiza for handling the TMAF microscope, to Cristina Madrid for DNA isolation, to Johnson Matthey for supplying K_2PdCl_4 and K_2PtCl_4 and to DGICYT (ref. PB94-0922-C02) for financial support.

REFERENCES

1 Rosenberg,B., Van Camp,L., Trosko,J.E. and Mansour,V.H. (1969) *Nature*, **222**, 385–386.
2 Farrell,N. (1989) *Transition Metal Complexes as Drugs and Chemotherapeutic Agents*. Kluwer Academic Publishers, Dordrecht, The Netherlands.
3 Keppler,B.K.(ed) (1993) *Metal Complexes in Cancer Chemotherapy*, VHC, Weinheim, Germany.
4 Wagstaff,A.J., Ward,A., Benfield,P. and Heel,R.C. (1989) *Drugs*, **37**,162–190.
5 Barton,J.F. (1995) In Bertini,I, Gray,H.B., Lippard,S.J. and Valentine,J.S. (eds), *Inorganic Biochemistry*. University Science Books, Mil Valley, CA, pp. 455–503.
6 Fichtinger-Schepman,A.M.J., van der Veer,J.L., den Hartog,J.H.J., Lohman,P.H.M. and Reedijk,J. (1985) *Biochemistry*, **24**, 707–713.
7 Lippard,S.J.(1995) In Bertini,I., Gray,H.B., Lippard,S.J. and Valentine,J.S. (eds), *Inorganic Biochemistry*. University Science Books, Mil Valley, CA, pp. 505–583.
8 Johnson,N.P., Butour,J.L., Villani,G., Wimmer,F.L., Defais,M., Pierson,V. and Brabec,V. (1989) *Prog. Clin. Biochem. Med*., **10**, 1–24.
9 Lepre,C.A. and Lippard,S.J. (1990) In Eckstein,F. and Lilley,D.M.J. (eds), *Nucleic Acids and Molecular Biology*. Springer Verlag, Berlin, Germany, Vol. 4, pp. 9–38.
10 Fichtinger-Schepman,A.M.J., Oosterom,A.T., Lohman,P.H.M.and Berends,F. (1987) *Cancer Res*., **47**, 3000–3004.
11 Pil,P. and Lippard,S.J. (1997) In Bertino,J.R.(ed.), *Encyclopedia of Cancer*. Academic Press, New York, NY, Vol. I., pp. 392–410.
12 Dijt,F.J., Fichtinger-Schepman,A.M.J., Berends,F. and Reedijk,J. (1988) *Cancer Res*., **48**, 6058–6062.
13 Prestayko,A.W., Crooke,S.T. and Carter,S.K. (eds) (1980) *Cisplatin: Current Status and New Developments*. Academic Press, New York, NY.
14 Sherman,S.E., Gibson,D., Wang,A.H.J. and Lippard,S.J. (1985) *Science*, **230**, 412–417.
15 Takahara,P.M., Rosenzweig,A.C., Frederick,C.A. and Lippard,S.J. (1995) *Nature*, **377**, 649–652.
16 Cohem,G.L., Baver,W.R., Barton,J.K. and Lippard,S. (1979) *Science*, **203**, 1014–1016.
17 Macquet,J.P. and Butour,J.L. (1978) *Biochimie*, **60**, 901–914.
18 Mong,S., Daskal,Y., Prestayko,A.W. and Crooke,S.T. (1981) *Cancer Res*., **41**, 4020–4026.
19 Jeffrey,A.M., Jing,T.W., DeRose,J.A., Vaught,A., Rekesh,D., Lu,F.X. and Lindsay,S.M. (1993) *Nucleic Acids Res*., **21**, 5896–5900
20 Rampino,N.J. (1992) *Biochem. Biophys. Res. Commun*., **182**, 201–207.
21 Carter,S.K. and Hellman,K. (eds) (1985) *Cancer Treatment Rev*., **12** (suppl. A).
22 Sykes,A.G. (1988) *Platinum Metals Rev*., **32**, 170–178.
23 Farrell,N. (1996) In Sigel H. (ed.), *Metal Ions in Biological Systems*., Vol. 32, Marcel Dekker, New York, NY. pp. 603–639.
24 Coluccia,M., Nassi,A., Loseto,F., Boccarelli,A., Mariggio,M.A., Giordano,D., Intini,F.P., Caputo,P. and Natile,G. (1993) *J. Med. Chem*., **36**, 510–512.
25 Atwell,G.J., Baguley,B.C. and Denny,W.A. (1989) *J. Med. Chem*., **32**, 396–401.
26 Kelland,L.R., Barnard,C.F.J., Mellish,K.J., Jones,M., Goddard,P.M., Valenti,M., Bryant,A., Murrer,B.A. and Harrap,K.R. (1994) *Cancer Res*., **54**, 5618–5623.
27 Sampedro,F., Ruiz van Haperen,V.W.T., Izquierdo,M.A., Vicens,M., Santaló,P., Pueyo,M., Llagostera,M., Marcuello,E. and De Andres,L. (1995) *Eur. J. Med. Chem*., **30**, 497–502.
28 Cervantes,G., Moreno,V. and Prieto,M.J. (1997) *Metal Based Drugs*, **4**, 9–18.
29 Moreno,V., Cervantes,G., Onoa,G.B., Sampedro,F., Santaló,P., Solans,X. and Font-Bardía,M. (1997) *Polyhedron*, **16**, 4297–4303.
30 Shao,Z., Mou,J., Czajkowsky,D.M., Yang,J. and Yuan,J.Y. (1996) *Adv. Phys*., **45**, 1–86.
31 Martin,L.D., Vesenka,J., Henderson,E. and Dobbs,D.L. (1995) *Biochemistry*, **34**, 4610–4616.
32 Yang,J. and Shao,Z. (1995) *Micron*, **26**, 35–49.
33 Bustamante,C. and Rivetti,C. (1996) *Annu. Rev. Biophys. Biomol. Struct*., **25**, 395–429.
34 Hansma,H.G. and Hoh,J.H. (1994) *Annu. Rev. Biophys. Biomol. Struct*., **23**, 115–139.
35 Bustamante,C., Vesenka,J., Tang,C.L., Rees,W., Guthod,M. and Keller,R. (1992) *Biochemistry*, **31**, 22–26.
36 Hansma,H.G., Sinsheimer,R.L., Li,M.Q. and Hansma,P.K. (1992) *Nucleic Acids Res*., **20**, 3585–3590.
37 Schaper,A., Pietrasanta,L.I. and Jovin,T.M. (1993) *Nucleic Acids Res*., **21**, 6004–6009.
38 Radmacher,M., Fritz,M., Hansma,H.G. and Hansma,P.K. (1994) *Science*, **265**, 1577–1579.
39 Bezanilla,M., Drake,B., Nudler,E., Kashlev,M., Hansma,P.K. and Hansma,H.G. (1994) *Biophys. J*., **67**, 2454–2459.
40 Hansma,P.K., Cleveland,J.P., Radmacher,M., Walters,D.A., Hillner,P.E., Bezanilla,M., Fritz,M., Vie,D., Hansma,H.G., Prater,C.B. *et al*. (1994) *Appl. Phys. Lett*., **64**,1738–1740.
41 Hansma,H.G., Sinsheimer,R.L., Groppe,J., Bruice,TC., Elings,V., Gurley,J., Bezanilla,M., Mastrangelo,I.A., Hough,P.V.C. and.Hansma,P.K. (1993) *Scanning*, **15**, 296–299.
42 Scherman,S.E. and Lippard,S. (1987) *Chem. Rev.* **87**, 1153–1181.
43 Bezanilla,M., Manne,S., Laney,D.E., Lyubchenko,Y.L. and Hansma,H.G. (1995) *Langmuir*, **11**, 655–650.
44 Hansma,H.G., Browne,K.A., Bezanilla,M. and Bruice,T.C. (1994) *Biochemistry*, **33**, 8436–8441.
45 Vesenka,J., Guthold,M., Tang,C.L., Keller,D., Delaine,E. and Bustamante,C. (1992) *Ultramicroscopy*, **42**, 1243–1249.
46 Watson,J.D., Hopkins,N.H., Roberts,J.W., Steitz,J.A.and Weiner,A.M. (1988) *Molecular Biology of the Gene*, 4th Edn. Benjamin/Cummings Publishing, Menlo Park, CA, p. 249
47 Thundat,T., Allison,D.P.and Warmack,R.J. (1994) *Nucleic Acids Res*., **22**, 4224–4228
48 Hansma,H.G., Bezanilla,M., Zenhausern,F., Adrian,M. and Sinsheimer,A. (1993) *Nucleic Acids Res*., **21**, 505–512.
49 Perez,J.M., Navarro-Ranninger,M.C., Requena,J.M., Jiménez-Ruiz,A., Parrondo,E. López,M.C. and Alonso,C. (1991) *Chemico-Biol. Interact*., **77**, 341–343.
50 Ciccareli,R.B., Solomon,M.J., Varshauski,A. and Lippard,S. (1985) *J. Biochem*., **24**, 7533–7537.
51 Roberts,J.J. and Friedlos,F. (1987) *Cancer Res*., **47**, 31–35.
52 Butour,J.L. and Johnson,N.P. (1986) *Biochemistry*, **25**, 4539–4543.
53 Eastman,A. and Barry,M.A. (1987) *Biochemistry*, **26**, 3303–3307.